ChemComm

ROYAL SOCIETY OF CHEMISTRY

COMMUNICATION

View Article Online
View Journal | View Issue

Cite this: *Chem. Commun.*, 2026, **62**, 2682

Received 13th November 2025,
Accepted 24th December 2025

DOI: 10.1039/d5cc06434a

rsc.li/chemcomm

Molecular communication system using Zn^{2+} selective supramolecular nanochannel to induce photoregulated catalysis

Soumya Srimayee,†[a] Biswa Mohan Prusty,†[a] Mrinal Kanti Kar,[a] Mathias Winterhalter*[bc] and Debasis Manna *[a]

We developed synthetic ionophores that self-assemble into supramolecular nanochannels for the transport of Zn^{2+} across lipid bilayers. The translocated Zn^{2+} forms a photoactive PPIX–Zn^{2+} complex that generates $^1O_2$ to oxidize tryptophan, establishing a Zn^{2+}-mediated cascade reaction network within confined spaces, which is crucial for developing photoregulated molecular communication systems.

Cellular communication, facilitated by transport proteins and ion channels, is essential for coordinating cellular activities and maintaining homeostasis. Several key biological functions, such as differentiation, apoptosis, and proliferation through ligand-receptor interactions and secondary messengers, are regulated by these transport proteins and ion channels.[1,2] Inspired by natural processes, molecular communication systems have emerged as an innovative approach to mimic cellular pathways using synthetic biomolecule-based nanochannels capable of transmitting and amplifying chemical signals across membranes. Such artificial ion transport-based systems not only enable precise spatiotemporal control of information exchange but also offer intelligent platforms for targeted therapy, biosensing, and synthetic cell-to-cell communication, thereby enhancing our understanding of stimulus-driven biochemical processes signalling.[3–7]

Recent studies have demonstrated the development of inter-vesicle and transmembrane signalling systems capable of transmitting signals with or without directly transferring ions or signalling molecules.[6,8] However, a significant limitation of these systems is the lack of controllability once mass transport across the membrane triggers a downstream chemical reaction.[9] Hence, introducing a stimulus-responsive communication system that regulates ion transport-mediated chemical reaction through external cues is crucial and presents a unique opportunity for understanding complex cellular signalling processes.[5,7] Transition metal ions, such as Zn^{2+}, play a pivotal role in many signalling processes, including enzyme activation, DNA synthesis, and immune regulation.[10] Hence, Zn^{2+} acts as an ideal cofactor for developing a controllable, biomimetic communication system. Inspired by the importance of Zn^{2+} in cellular environments, we developed a photo-responsive molecular communication system by integrating a synthetic ion transporter with a protoporphyrin IX (PPIX) (Fig. 1). The 2-(pyridin-2-yl)-1*H*-benzo[*d*]imidazol-6-amine-based tripodal compound (**3d**) self-assembled to form supramolecular nanochannels within the lipid bilayers to selectively transport Zn^{2+} from the extravesicular to the intravesicular environment. The complexation of transported Zn^{2+} with the PPIX resulted in the formation of a catalytic system to promote singlet oxygen ($^1O_2$)-mediated oxidation of tryptophan (Trp) amino acid to

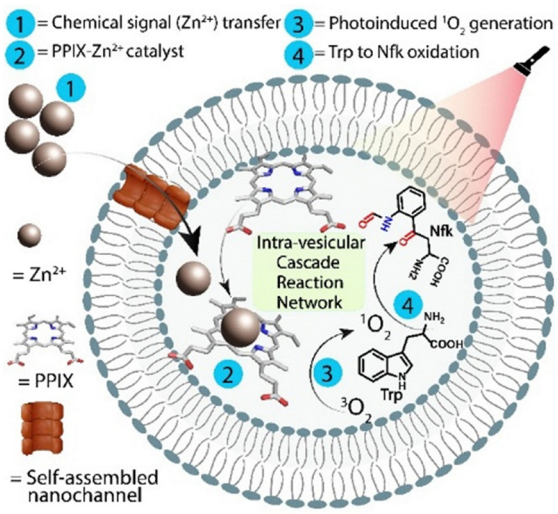

Fig. 1 A schematic representation of the molecular communication process *via* Zn^{2+} transport, facilitating *in situ* complexation of Zn^{2+} with PPIX, which leads to reactive oxygen species (ROS) generation and the subsequent oxidation of Trp to Nfk.

[a] *Department of Chemistry, Indian Institute of Technology Guwahati, Guwahati, Assam, India. E-mail: dmanna@iitg.ac.in*
[b] *Institute for Nanostructure and Solid-State Physics, University of Hamburg, Luruper Chaussee 149, 22761, Hamburg, Germany*
[c] *School of Science, Constructor University, Campus Ring 1, 28759, Bremen, Germany*
† S. S. and B. M. P. contributed equally.

N-formyl kynurenine (Nfk) exclusively in the presence of light within the intravesicular environment. Therefore, this molecular communication system utilizes synthetic ion transporters for transferring encrypted chemical signals and employs PPIX and red light for decryption through biochemical transformations, thereby providing a modular strategy for designing programmable protocells.

The 2-(pyridin-2-yl)-1*H*-benzo[*d*]imidazole is a known sensor of Zn^{2+}, particularly due to the interaction between the imidazole and pyridyl nitrogen atoms with the Zn^{2+}.[11] However, due to its lower lipophilicity (log *P* 1.95), it cannot be directly used as a transmembrane transporter of Zn^{2+}. Hence, to develop potent transmembrane Zn^{2+} transporters, we synthesized tripodal and dipodal thiourea derivatives of 2-(pyridin-2-yl)-1*H*-benzo[*d*]imidazole. The reactions of 1,3,5-triethyl-2,4,6-tris-(isothiocyanatomethyl)benzene with 2-(pyridin-2-yl)-1*H*-benzo[*d*]imidazol-6-amine and other aryl amines yielded **3a–3d** (Fig. 2). The reactions of 1,3-bis(isothiocyanatomethyl)-benzene with 2-(pyridin-2-yl)-1*H*-benzo[*d*]imidazol-6-amine and 2-(1*H*-pyrrol-2-yl)-1*H*-benzo[*d*]imidazol-6-amine resulted in the formation of dipodal **5a.** Compounds **3a**, **3b**, and **5a** were synthesized to investigate the role of thiourea, 2-(pyridin-2-yl)-1*H*-benzo[*d*]imidazole, and tripodal moieties in Zn^{2+} transport.

The ion transport aptitude of the synthesized compounds was evaluated using the large unilamellar vesicles (LUVs) of egg yolk phosphatidylcholine (EYPC) and cholesterol (Chol) (8 : 2 molar ratio) by encapsulating pentapotassium salt of magnesium green (MgG) (Fig. 3A).[12] The LUVs were prepared in 10 mM HEPES buffer containing 100 mM NaCl, 50 μM MgG, and 100 μM EDTA at pH 7.0. The compound screening assay showed higher Zn^{2+} transport efficacy for **3d** (~75%) compared to its related derivatives, **3a–3c** and **5a**, highlighting it as a promising candidate for further investigation and potential applications (Fig. 3B). The lower Zn^{2+} transport efficacy of **3c** and **5a** in comparison to **3d** suggests the importance of the 2-(pyridin-2-yl)-1*H*-benzo[*d*]imidazole and tripodal moieties in Zn^{2+} recognition and transport.

The concentration-dependent MgG assay of **3d** showed a half-maximal effective concentration (EC_{50}) of 44.83 ± 1.74 nM (**3d**: lipid = 1 : 5 × 10^5) and the Hill coefficient (*n*) value of 1.87 ± 0.09 (Fig. S1). The Hill coefficient value (~2) suggests that **3d** exhibits positive cooperativity in forming supramolecular channels within the lipid bilayers.[13] The cation selectivity study

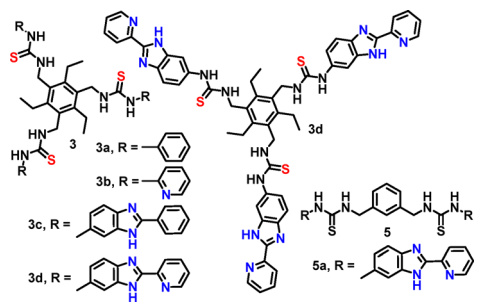

Fig. 2 Structure of the synthesized compounds.

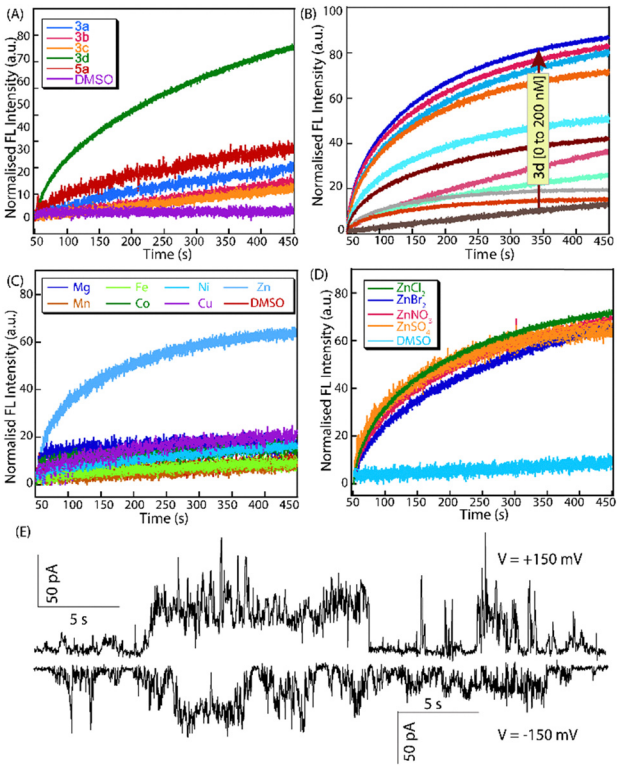

Fig. 3 (A) Evaluation of the Zn^{2+} transport activity of the synthesized compounds (40 nM) across EYPC/Chol-LUVs⊃MgG (B) Concentration-dependent Zn^{2+} transport activities of **3d**. (C) Cation and (D) anion transport selectivity of **3d** (40 nM) across EYPC/Chol-LUVs⊃MgG. (E) Ion conductance measurements across the BLM at +150 mV and −150 mV in the presence of **3d** in a symmetrical solution of $ZnCl_2$ (0.5 M) in water.

performed for **3d** revealed the selectivity for Zn^{2+} among the tested cations (Fig. 3C). Additionally, for monovalent cations, the transport study was performed using EYPC/CHOL-LUVs⊃HPTS, which showed negligible transport by **3d** (Fig. S3). However, no difference in Zn^{2+} transport efficacy was observed in anion selectivity studies (Fig. 3D). Minimal but measurable Cl^- transport activity (~20%) was observed, but this activity is considerably lower than its Zn^{2+} transport activity (Fig. S4). The sulfur atom of the thiourea moiety is known to interact with Zn^{2+} and other metal ions.[14] The UV-Vis-based titration study revealed the binding constant of 7439 ± 3 M^{-1}, suggesting a moderate affinity of **3d** for Zn^{2+} (Fig. S5). The ^{1}H NMR-based interaction studies clearly showed that the benzimidazole NH proton showed a strong interaction with the Zn^{2+}, and a partial shift of thiourea NH suggests that Zn^{2+} weakly interacts with the thiourea group (S atom of the thiourea group) (Fig. S6 and S7).

Mechanistic studies using MgG-encapsulated liposomes were conducted in the presence of FCCP (H^+ carrier) and valinomycin (K^+ uniporter).[9] No notable change in MgG fluorescence was observed with or without FCCP, suggesting H^+ participation in **3d**-mediated Zn^{2+} transport (Fig. S8). Further, pH-sensitive fluorescein assays showed increased fluorescence across EYPC/CHOL-LUV⊃fluorescein, confirming H^+ efflux (Fig. S9).

Thus, both FCCP and fluorescein assays established the Zn^{2+}/H^{+} antiport activity of **3d**. Valinomycin-based studies showed unchanged transport efficiency with or without the K^{+} uniporter, indicating no OH^{-} involvement (Fig. S10). The carboxyfluorescein leakage assay confirmed no vesicle disruption (Fig. S11). To probe the transport pathway, Chol-dependent and U-tube assays were performed. LUVs with EYPC: CHOL ratios of 6 : 4 and 8 : 2 showed no change in activity, supporting a channel-based mechanism (Fig. S12). In the U-tube assay, **3d** failed to transport Zn^{2+} across the nonpolar phase, unlike clioquinol, a known Zn^{2+} carrier (Fig. S13).

The FESEM images revealed that **3d** formed nanowire-like structures in a hydrophobic environment (chloroform) and exhibited spherical agglomeration in a hydrophilic medium (water), indicating solvent-dependent self-assembly (Fig. S14). The 2D-NOESY measurement of **3d** revealed a strong spatial correlation between the pyridyl aromatic proton (δ 7.51 ppm) and the thiourea N–H proton (δ 9.49 ppm) (Fig. S15). Additionally, cross-peaks were observed between the benzylic proton (δ 4.68 ppm) and the ethyl group proton (δ 2.80 ppm) with the pyridyl aromatic proton (δ 7.49 ppm). These interactions suggest a self-assembled architecture in which pyridyl arms interlock *via* noncovalent interactions, while the remaining arms form a channel-like cavity.

To further investigate the channel-forming ability, the real-time change in current at a constant voltage in the presence of **3d** was monitored through an electrophysiological experiment.[15] After the addition of **3d** (4 μM) to both chambers, we observed repetitive opening-closing events at various holding potentials, confirming the formation of an ion channel within the planar lipid bilayer (Fig. 3E and Fig. S16). Additional measurements of current against voltage (*I–V* plot) were further monitored using a symmetrical $ZnCl_2$ (0.5 M) solution (Fig. S17). A linear increase in current was noted with increasing voltage, indicating the ohmic behavior. The measured single-channel conductance (G) of 54 ± 11 pS indicates the formation of ion channels with a pore diameter of approximately 1.5 Å.

Metalloporphyrins are essential biomolecules with catalytic properties that play vital roles in physiological functions within living systems. Metalloporphyrins are also used in molecular catalysis, water splitting, and photodynamic therapy.[16,17] The zinc-porphyrin has been identified as a ROS generator under photo-irradiation,[18] which can be utilized for carrying out reactions within the compartmentalized structures, such as LUVs. We observed that the complexation between PPIX and Zn^{2+} leads to the generation of ROS when exposed to red light. The enhancement of fluorescence intensity at 522 nm due to the conversion of 7′-dichlorofluorescin diacetate (H_2DCFDA) to 2′,7′-dichlorofluorescein (DCF) was only observed in the presence of both PPIX and Zn^{2+} upon photo irradiation (Fig. S18). No significant DCF fluorescence enhancement was observed with PPIX alone, indicating that Zn^{2+} binding significantly enhances the ROS generation aptitude of PPIX. The UV-Vis and fluorescence-based titration studies of PPIX with Zn^{2+} showed no metalation of PPIX (Fig. S19 and S20). All four Q bands (500–700 nm) of PPIX remained intact, suggesting no Zn^{2+} incorporation into the porphyrin ring of PPIX.[19] However, a partial decrease in the Soret band (400 nm) and a significant reduction in fluorescence intensity at 640 nm indicated either complexation of Zn^{2+} with the carboxylate groups of PPIX or adopting a weakly bound, 'sitting-atop' geometry above the porphyrin ring, without coordination to the core nitrogen atoms. These Zn^{2+} binding modes may significantly alter the electronic structure of the porphyrin ring, thereby enhancing the ability to generate ROS upon photoactivation.[18]

To investigate the ROS-mediated catalytic activities of PPIX-Zn^{2+} complex, the reactions were performed in the presence of Trp amino acid, both with and without light, in a 20 mM HEPES buffer at pH 7.0 (Fig. S21). Upon optimization, we observed that red light achieves better photo-oxidation in just 3–4 h, whereas white light requires approximately 24 h to reach similar efficiency, highlighting the superior effectiveness of wavelength-specific excitation for Zn^{2+}-PPIX-mediated photo-oxidation. Additionally, exposure to white light can promote increased nonspecific photodegradation of Zn^{2+}-PPIX, reducing its effectiveness, as confirmed by HPLC analysis (Fig. S22).

Interestingly, after 4 h of red-light exposure, the HRMS analysis detected the formation of Nfk ($[M + H]^{+}$ = 237.0905) only in the reaction mixture containing Trp and PPIX-Zn^{2+}. Nfk is known to undergo hydrolysis to kynurenine (Kyn) in the presence of trichloroacetic acid (TCA).[20,21] The resulting Kyn was subsequently quantified using UV-Vis spectroscopy following derivatization with *p*-dimethylaminobenzaldehyde (*p*-DMAB). The UV-Vis spectral analysis revealed a significant enhancement of the peak at 480 nm, which corresponds to the formation of the imine complex of *p*-DMAB with Kyn (Fig. S18).[20] The time-dependent HPLC analysis confirmed increasing Kyn formation with light exposure, while no significant amount of Kyn was detected without light (Fig. S23).

The HRMS and NMR analysis of the eluted solution confirm the identity of Kyn (Fig. S24 and S25). Additional reactions of Trp with the PPIX-Zn^{2+} complex in the presence of different ROS quenchers were performed to investigate the Trp-to-Kyn formation mechanism. DABCO, known as a $^1O_2$ scavenger, suppressed both HPLC and absorbance peaks, suggesting the conversion of Trp to Kyn proceeds *via* $^1O_2$ under light (Fig. S26).[22] Additional photo-regulated oxidation studies using the PPIX-Zn^{2+} complex with tyrosine revealed its dimerization, while with methionine, it demonstrated mono-oxidation to methionine sulfoxide (Table S2 and Fig. S27).

This finding provided a unique opportunity to develop a photo-regulated, Zn^{2+}-dependent molecular communication system. The EYPC/Chol-LUV⊃PPIX/Trp were prepared in 20 mM HEPES buffer at pH 7.0. The LUVs were suspended in 20 mM HEPES buffer at pH 7.0, and **3d**, along with Zn^{2+}, was added to the extravesicular solution (Fig. 4A). After prolonged exposure (4 h) to the red lights, the LUVs were lysed using 20% Triton X-100 (20 μL) (Fig. S28). The HPLC and UV-Vis spectral analysis suggested the conversion of Trp to Kyn under the vesicular environment. Control experiments without **3d**, Zn^{2+}, Tyr, or light showed no significant formation of Kyn. The time-resolved HPLC analysis confirmed a gradual increase in the Kyn formation, supporting Kyn formation *via* transmembrane Zn^{2+}

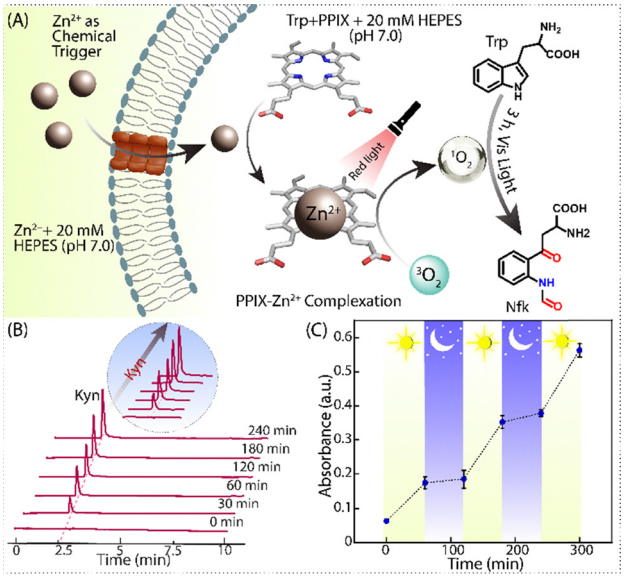

Fig. 4 (A) A schematic illustration shows the *in situ* complexation of Zn^{2+} with PPIX, initiating light-regulated catalysis that significantly increases the generation of ROS and leads to the oxidation of Trp to Nfk. (B) HPLC analysis at different time intervals demonstrates the production of Kyn within the EYPC/Chol-LUVs⊃Trp/PPIX system after photo-irradiation in the presence of **3d** and Zn^{2+}. (C) Stepwise red-light irradiation ON/OFF experiment using EYPC/Chol-LUVs⊃Trp/PPIX in 20 mM HEPES buffer, pH 7.0, with **3d** and Zn^{2+} to detect Kyn generation.

transport by **3d** and $^1O_2$-mediated oxidation under light within a confined vesicular environment (Fig. 4B). We also conducted a similar reaction under alternating 60 min light and dark cycles for a total duration of 300 min. The HPLC and UV-Vis spectral analysis showed that light-dependent Trp to Kyn conversion is associated with the photo-induced $^1O_2$ generation by the *in situ* generated PPIX-Zn^{2+} complex within the vesicles (Fig. 4C and Fig. S29). The indoleamine-2,3-dioxygenase (IDO1) enzyme-mediated catabolism of Trp to Nfk through the kynurenine pathways is involved in various physiological processes, including the immune response.[20,21] Hence, this photo-regulated molecular communication system functions as an artificial enzyme to mimic the catalytic conversion of Trp to Nfk.

In conclusion, we developed an ion transport-mediated photo-responsive molecular communication system. The self-assemblies of **3d** within the bilayer form supramolecular channels that transport Zn^{2+} along with H^+ in an antiport manner. Due to the selective Zn^{2+} transport ability of **3d**, Zn^{2+} was utilized as a chemical signal to form Zn^{2+}-PPIX complex, a photosensitizer, within the vesicular environment. The PPIX-Zn^{2+} complex showed $^1O_2$-mediated enzyme-like oxidation of Trp to Nfk within the vesicles. Hence, this molecular communication system presents a unique biomimetic approach where Zn^{2+} serves not only as a transportable ion but also as a functional chemical signal that triggers an enzyme-like oxidation reaction exclusively under red light.

Conflicts of interest

There are no conflicts to declare.

Data availability

Supplementary information (SI): detailed experimental procedures, compound characterization, and ion transport activity data, and catalytic activity data were included. See DOI: https://doi.org/10.1039/d5cc06434a.

Acknowledgements

The authors acknowledge the SERB (CRG/2021/000306) and DBT (BT/PR52583/NER/95/2189/2024) New Delhi, India, for financial support, New Delhi, India, for financial support. The authors also recognize the instrumental facilities provided by the Central Instrument Facility (CIF) and the Department of Chemistry at IIT Guwahati. DM acknowledges DAAD for the Research Stays fellowship.

References

1 J. Su, Y. Song, Z. Zhu, X. Huang, J. Fan, J. Qiao and F. Mao, *Signal Transduction Targeted Ther.*, 2024, **9**, 196.
2 M. Mustafa, R. Ahmad, I. Q. Tantry, W. Ahmad, S. Siddiqui, M. Alam, K. Abbas, M. I. Hassan, S. Habib and S. Islam, *Cells*, 2024, **13**, 1838.
3 K. Shi, C. Song, Y. Wang, R. Chandrawati and Y. Lin, *Commun. Mater.*, 2023, **4**, 65.
4 J. Wang, M. Xie, L. Ouyang, J. Li, L. Wang, C. Fan and J. Chao, *Nat. Commun.*, 2025, **16**, 244.
5 M. J. Langton, F. Keymeulen, M. Ciaccia, N. H. Williams and C. A. Hunter, *Nat. Chem.*, 2017, **9**, 426–430.
6 M. J. Langton, L. M. Scriven, N. H. Williams and C. A. Hunter, *J. Am. Chem. Soc.*, 2017, **139**, 15768–15773.
7 M. J. Langton, N. H. Williams and C. A. Hunter, *J. Am. Chem. Soc.*, 2017, **139**, 6461–6466.
8 S. A. Gartland, T. G. Johnson, E. Walkley and M. J. Langton, *Angew. Chem., Int. Ed.*, 2023, **62**, e202309080.
9 S. Srimayee, B. M. Prusty, M. K. Kar, M. Winterhalter and D. Manna, *Angew. Chem.*, 2025, **64**, e202501634.
10 B. Chen, P. Yu, W. N. Chan, F. Xie, Y. Zhang, L. Liang, K. T. Leung, K. W. Lo, J. Yu and G. M. Tse, *Signal Transduction Targeted Ther.*, 2024, **9**, 6.
11 R. Schiffmann, A. Neugebauer and C. D. Klein, *J. Med. Chem.*, 2006, **49**, 511–522.
12 B. M. Prusty, S. Srimayee, R. Karn, N. Haloi, S. K. Singh, M. Winterhalter and D. Manna, *Chem. – Eur. J.*, 2025, **31**, e202501013.
13 R. Paul, D. Dutta, T. K. Mukhopadhyay, D. Müller, B. Lala, A. Datta, H. Schwalbe and J. Dash, *Nat. Commun.*, 2024, **15**, 5275.
14 M. Muhammad, S. Khan, S. A. Shehzadi, Z. Gul, H. M. Al-Saidi, A. W. Kamran and F. A. Alhumaydhi, *Dyes Pigm.*, 2022, 205.
15 T. Gutsmann, T. Heimburg, U. Keyser, K. R. Mahendran and M. Winterhalter, *Nat. Protoc.*, 2015, **10**, 188–198.
16 X. Li, H. Lei, L. Xie, N. Wang, W. Zhang and R. Cao, *Acc. Chem. Res.*, 2022, **55**, 878–892.
17 S. S. Rajasree, X. Li and P. Deria, *Commun. Chem.*, 2021, **4**, 47.
18 A. S. Lavado, V. M. Chauhan, A. A. Zen, F. Giuntini, D. R. E. Jones, R. W. Boyle, A. Beeby, W. C. Chan and J. W. Aylott, *Nanoscale*, 2015, **7**, 14525–14531.
19 A. Restrepo-Acevedo, M. I. Murillo, C. Orvain, C. Thibaudeau, S. Recberlik, L. Verget, V. G. Vidales, C. Gaiddon, G. Mellitzer and R. Le Lagadec, *Inorg. Chem.*, 2025, **64**, 9684–9702.
20 N. Pradhan, N. Akhtar, B. Nath, J. Peña-García, A. Gupta, H. Pérez-Sánchez, S. Kumar and D. J. C. C. Manna, *Chem. Commun.*, 2021, **57**, 395–398.
21 S. Paul, A. Roy, S. J. Deka, S. Panda, V. Trivedi and D. Manna, *Eur. J. Med. Chem.*, 2016, **121**, 364–375.
22 M. Grigalavicius, M. Mastrangelopoulou, K. Berg, D. Arous, M. Ménard, T. Raabe-Henriksen, E. Brondz, S. Siem, A. Görgen and N. F. J. Edin, *Nat. Commun.*, 2019, **10**, 3986.